Road Slope Estimation with Standard Truck Sensors

Ken Johansson

Master Thesis
Department of Signals, Sensors and Systems
KTH

2005-04-25

Abstract

Several recent studies have examined the possibilities for more intelligent control of the vehicle by using knowledge of road slope data. As three-dimensional navigational road maps are not commercially available today the road slope has to be measured. This report focuses on the ability to estimate the road slope in a standard Scania truck, without any additional sensors. Information from GPS receiver, pressure sensor and torque sensor were used. By modelling the trucks movement and applying an extended Kalman filter an estimation of the road slope was achieved. The three sensors were evaluated to find specific characteristics. Each of them were tested through a stability and an absolute accuracy perspective. The results showed different sensor characteristics with warring stability and accuracy. Additionally a short assessment of the sampling distance was carried out.

Acknowledgment

This Masters Thesis work has been carried out between October 2004 and April 2005 at Scania CV AB in Södertälje.

First of all I would like to extend my thanks to my supervisor at Scania, Tony Sandberg. He has been very helpful and has guided me through the project's twist and turns. I would also like to thank my supervisor Karl Henrik Johansson at KTH, associate professor at the department of Signals, Sensors and Systems, for helpful concepts and ideas. I would further like to thank Henrik Jansson for his knowledge and good suggestions. Finally I would like to thank everyone at Scania involved during this project and all members at the RESC department for their support and for making my time at Scania most enjoyable.

Södertälje, April 2005
Ken Johansson

Notation

Symbols

a	Acceleration
A	System matrix
B	System input matrix
F_{air}	Air resistance
F_{drive}	Driving resistance
$F_{gravity}$	Gravitational force
$F_{incline}$	Incline force
F_{roll}	Rolling resistance
F_{torque}	Engine torque force
g	Gravitational acceleration
H	Measurement matrix
I	Identity matrix
K	Kalman gain
m	Vehicle mass
p	Barometric pressure
P	Estimate error covariance matrix
Q	Process noise covariance matrix
r	Earth radius
R	Measurement noise covariance matrix
s	Distance
T	System sample time
u	System input
v	Measurement noise

V	Measurement noise matrix
w	Process noise
W	Process noise matrix
x	State vector
$\hat{x}$	Estimate of state vector
$\widetilde{x}$	Approximate state vector
y	Measurement vector
$\widetilde{y}$	Approximate measurement vector
z	Altitude
α	Road slope angle
γ	Conversion factor from atmospheric pressure to altitude
ς	Conversion factor from radians to percent
σ	Standard deviation

Operators and functions

E	Expected value
f	System function
h	Measurement function
V	Variance

Abbreviations

3D	Three Dimensional
ADASIS	Advanced Driver Assistance Systems Interface Specification
ASCII	American Standard Code for Information Interchange
CAN	Controller Area Network
CEP	Circular Error Probability
DGPS	Differential GPS
EKF	Extended Kalman Filter
GNSS	Global Navigation Satellite System
GPRS	General Packet Radio Services
GPS	Global Positioning System
GSM	Global System for Mobile telecommunications
Hz	Hertz
ITS	Intelligent Transport Systems
km	Kilometre

KTH	Royal Institute of Technology (Kungliga Tekniska Högskolan)
MSL	Mean Sea Level
NMEA	National Marine Electronics Association
NVDB	National Road Database (Nationell Vägdatabas)
Pa	Pascal
PC	Personal Computer
SNRA	Swedish National Road Administration
std	Standard deviation
UTC	Coordinated Universal Time

Contents

1 Introduction

1.1 Background

In the truck industry fuel consumption is of great importance. Drivers today drive on average 150 000 km each year [1] making fuel costs a major expense for haulage contractors. When customers invest in new trucks the total lifetime cost of the truck plays a very important role with low fuel consumption as a vital argument. This is why Scania is putting major efforts into making next generation trucks more and more fuel economic.

Techniques for lowering the overall fuel consumption using knowledge of the upcoming road-behaviour are under development. Several ways have been proposed in recent studies. In [2] an increase of the controllability of the cooling system in heavy vehicles is studied. The cooling system is today mechanically driven with a fix ratio to the engine speed resulting in excess capacity in most driving cases. By making the cooling fan and water pump electrically driven and control the output to the actual need the energy loss is shown to decrease, resulting in potentially lower fuel consumption. For optimal control the knowledge of future road condition is needed. [3] also discusses the potential of coordinated operation of vehicle auxiliary systems to decrease fuel consumption. The air condition and the diesel particle filter are studied. In the case of the diesel particle filter prediction of upcoming engine work load is required. This is obtained through knowledge of future road conditions. It is shown that a considerable decrease in fuel consumption can be obtained. In the area of powertrain control [4] proposes an adaptable cruise control system for stop and go situations on a congested road. Using values for required engine torque, gear and slope of road a reduction of the fuel consumption by approximately 3% is achieved.

Another proposed way to lower the fuel consumption is to extend the use of the conventional cruise control function even further into a predictive cruise control [5]. The basic idea is for the truck to climb and descend hills in an effective and fuel saving way. This is done by varying the speed around the cruise control set speed within a speed band. The system is based on elevation road information saved onboard with the combination of a predictive algorithm. The results show a diesel fuel saving of up to 3%. Similar studies have been done in [6] and [7] with fuel savings of 2% or more, depending on the route topography.

All these proposed fuel saving techniques are dependent on the knowledge of how the road ahead will behave, especially the topographical character. A technique to derive this information is obviously necessary. This project therefore focuses on the accessibility and processing of elevation and slope data for roads travelled by heavy trucks. It is to be used primarily for applications with cruise control and predictive algorithms.

Ways to estimate road slope have been proposed in many papers. In [8] road slope is measured by GPS. Two methods are explained, the first one with a two antenna setup and the other with one antenna. The two antenna setup tracks the carrier phase at each antenna giving the angle relative the horizon. In the case of the one antenna setup the ratio of vertical to horizontal velocity is used to estimate road slope. Results show less oscillation caused by vehicle pitch in the velocity based estimation. [9] proposes an application of recursive least squares with multiple forgetting factors. The estimation relies on a model of the longitudinal vehicle dynamics. As for [10] Kalman filtering is used to obtain estimation of vehicle mass and road slope. Two sensor configurations are examined, one where speed is measured and one where both speed and specific force are measured. Results show that both sensor configurations are robust and accurate. Parameter estimation using Kalman filter has also been proposed by [11] and [12], although only in the horizontal plane for positioning purposes.

1.2 Objective and Goal

The objective of this Masters Thesis is to examine the possibility of retrieving topographical information about the upcoming road in front of the travelling truck. For this purpose two main sources of information are considered. One is to extract information from digital three-dimensional road maps provided by a third party company. The second one is to

automatically record the travelled road the first time the vehicle drives over it, making its own three-dimensional map for all of the truck's later journeys along the same route. After investigating which source is the most appropriate, the goal is to derive a possible technique that can be used for obtaining slope values for the upcoming road travelled by the truck. The system would mainly be intended for motorways and roads with higher speeds.

1.3 Outline

Chapter 2 discuss different ways for retrieving information about the topographical nature of roads. Different possible sources and methods are examined leading up to the road slope recording to be the most promising method.

In Chapter 3 the sensors and systems used for the slope estimation is described in detail. Each sensors capacity and limits are discussed. The experimental measurement collection procedure is also described together with a description of the reference road map received.

The theory behind the slope estimation is described in chapter 4. Here modelling and filtering is described together with a simple explanation of the relation between road altitude and slope.

Chapter 5 shows the implementation and the experimental results. A sensor evaluation was carried out to state each sensor's characteristic and to determine which sensor is the most reliable. In the end of this chapter a discussion about the sampling rate is also done.

The thesis is summed up in chapter 6 with conclusions, followed by the final discussion and possible future work in chapter 7.

2 Source of Information

As mentioned earlier, two main sources of information are considered for obtaining topographical information of a road, three-dimensional road maps and updatable road slope recordings of the travelled road. With future presumed digital three-dimensional road maps easy access to slope data through navigational data discs would be achieved. Drawbacks are the presumed high costs for the data and the assumed restriction to big motorways from where data is collected. Although more and more roads would be included over the years collecting data is a major task. The road slope recording would on the other hand mainly benefit from low costs. All sensors used for this purpose are already present on the truck and used for other tasks, meaning no extra cost for expensive digital maps are necessary. Weaknesses to this system are the probable short term lack in accuracy and the initial low coverage.

2.1 Three-Dimensional Road Maps

Although three-dimensional road maps are not commercially available today work is underway. In 2001 the leading supplier of navigational road maps Navteq initiated what later became ADASIS[1]. This is a forum under ERTICO, a multi-sector partnership pursuing the development and deployment of Intelligent Transport Systems and Services (ITS), with members from all major auto manufacturers and navigation suppliers. Here standards about road map attributes and data communication of future

[1] Advanced Driver Assistance Systems Interface Specification

digital road maps are discussed. Possibility to predict the road geometry with its related attributes ahead of the vehicle is of main interest.

But as no three-dimensional road maps are available today information on coming digital map standards were needed. A meeting with Daniel Stehn and Claes Nyqvist, both working with road navigation issues at Scania, was held in order to establish the digital road map situation of today and to forward questions to digital road map providers. Unfortunately it proved to be very difficult to attain information or test data for future three-dimensional maps. Instead another possible source of information was examined, the upcoming National Road Database (NVDB[2]). This is a joint venture between the Swedish National Road Administration (SNRA), the Central Office of the National Land Survey, the Swedish Association of Local Authorities, and the forest industry. The aim for this project is to establish a nationwide database containing up-to-date, quality-assured information on the entire Swedish road network. Here roads are saved with information in all three dimensions. But as NVDB is under construction no standard for the transfer of road data from the database to the customer was yet established. With no real map data to work from focus was turned to the road slope recording.

2.2 Road Slope Recording

For the road slope recording available sensors on the truck that could be used for recording the topographical image of the road were taken into consideration. The aim was to investigate the possibility to estimate the road slope with no additional sensors added. Three sensors were chosen. Information from GPS receiver, pressure sensor and torque sensor were

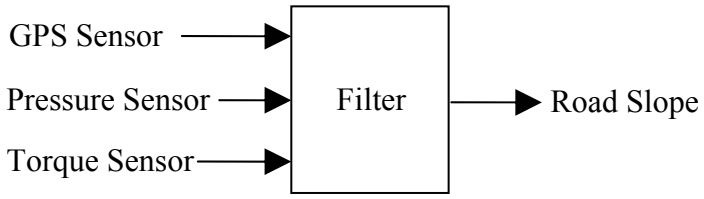

Figure 2.1: Sensor scheme.

[2]The abbreviation NVDB stands for Nationell Vägdatabas

used one at the time, shown in Figure 2.1. An estimation of the current road slope was to be done through a Kalman filter. As the accuracy from only one measurement run is not considered sufficient the measured roads have to be able to be updated so that higher accuracy is obtained as the road is passed several times.

2.3 Measurement Acquisition

Measurements were collected over two different types of road, one motorway segment and one main road segment. Both segments are roads between Södertälje and Strängnäs with the approximate distance of 50 km. Measurements were collected by driving a Scania R420 at normal traffic rhythm with air-conditioning system in automatic mode while recording sensor outputs from the three sensors. Each road type was measured four times at four different occasions adding up to a total of eight road measurements.

3 Sensors and Measurements

The outline for the project was to use existing sensors in a Scania truck for road slope estimation. The Scania R420 seen in Figure 3.1 was used during all measurements. The Scania R420 is a standard truck equipped with the option Scania Interactor 500 with built-in GPS receiver. Systems and sensors used for this research will be discussed further in this chapter. Also the measurement procedure and the reference road used are presented.

Figure 3.1: Scania R420 test vehicle.

3.1 GPS Sensor

The GPS receiver is integrated with the Scania Interactor 500 which is a fleet management tool. It is a platform including a full-powered PC with a 10.4 inch colour touch screen monitor. The PC runs on Microsoft Windows 2000 operating system and integrates software for Microsoft Windows, GSM/GPRS telecommunication and GPS capabilities for navigation and fleet management services [13]. The integrated GPS receiver is a μ-blox TIM GPS Receiver based on the SiRFstar™ II chip[3]. It is a fully self-contained receiver module with GPS signal processing from antenna input to serial data output [14]. The GPS information was logged and saved with GPS Diagnostics v1.05[4] run on the Interactor 500 platform. The information received from the GPS was in the form of NMEA sentence strings (see Appendix A). Latitude, longitude, altitude, number of used satellites and velocity were recorded with the frequency of 1 Hz.

The accuracy of a GPS receiver is not a well defined number. Every manufacturer has its own way of determining the accuracy mainly depending on satellite visibility of the antenna, antenna type, satellite constellation and receiver performance. The GPS used in this study, the μ-blox TIM GPS Receiver, has a horizontal accuracy of 4 meters CEP[5] [14]. The accuracy in the altitude measurement is reported to be 3-4 times worse than the horizontal accuracy leading to a vertical accuracy of somewhere between 12-16 meters, stated by the maker. The GPS receiver has a built in filter for smoothing measurements, but the receiver still incorporate the main GPS problem with areas of low or no satellite coverage. The antenna mounted on the cab roof was a Smarteq ANT antenna. It is a multifunction antenna including antennas for GPS and dual band mobile phone [15] which comes with the Interactor 500 package. Early tests showed big differences in altitude measurements from different types of antennas and proved to have a larger impact on the accuracy than the quality of the GPS receiver itself.

[3] Manufactured by SiRF Technology, Inc.
[4] Freeware GPS Diagnostic Program from CommLinx Solutions Pty Ltd.
[5] Circular Error Probability: The radius of a circle, centred at the antennas true position, containing 50% of the fixes.

3.2 Pressure Sensor

The pressure sensor, or barometer, monitored was a Motorola MPXA6115A [16] used for measuring surrounding barometric pressure to adjust engine air inlet. The barometric pressure measured by the sensor was available over the in-vehicle communications network CAN[6]. The resolution was predefined to 0.05 kPa/bit. At near ground level pressure drops 0.1 kPa every 8.4 meters rising vertically and with this conversion rate the altitude measurement resolution becomes 4.2 meters/bit. As the placing of this sensor is situated behind the dash board in the driver cab it is subjected, apart from weather influences, to pressure influences from the air-conditioning system. As no indicator of fan speed is available this influence is immeasurable. Barometric pressure data was received at 1 Hz.

3.3 Torque sensor

A third signal estimating the road slope was computed from the engine torque parameters. The calculation is based on the vehicle mass *m* and driving resistance. The vehicle mass is estimated through Newton's second law of motion

$$F_{torque} = ma \tag{4.1}$$

at certain instances so that the mass estimation becomes independent from the slope of the road. The force F_{torque} is derived from engine torque and the acceleration *a* is measured through wheel speed sensors. When the mass is established the driving resistance F_{drive} can be determined through

$$F_{drive} = F_{torque} - ma \tag{4.2}$$

where road slope now is taken into consideration. Two more forces are needed to be able to calculate road slope, incline force and gravitational force

$$F_{incline} = F_{drive} - F_{roll} - F_{air} \tag{4.3}$$

$$F_{gravity} = mg \tag{4.4}$$

[6] Controller Area Network

where F_{roll} is the rolling resistance derived from vehicle mass and velocity and F_{air} is the air resistance derived from vehicle velocity. The road slope can now be calculated as

$$\alpha = \arctan\left(\frac{F_{incline}}{F_{gravity}}\right), \tag{4.5}$$

according to Figure 3.2. There is one disadvantage with this way of estimating road slope. When wheel brakes are pressed the force of which they are acting on the vehicle is unknown. This causes an added unknown force to equation (4.3) making estimation of road slope not possible during use of wheel brakes. The calculation is then set to outputs a non-valid estimate in the form of a 13% positive incline value. Road slope was estimated and received at 10 Hz.

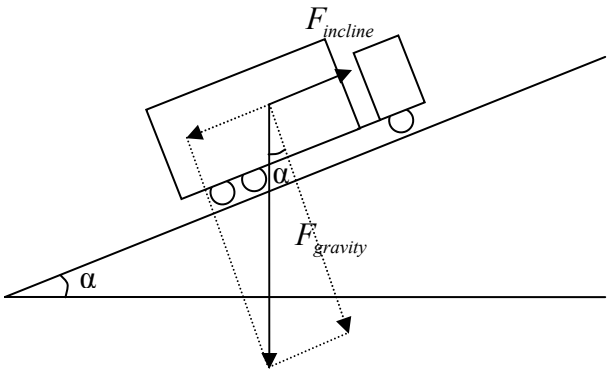

Figure 3.2: Calculated road slope estimation.

3.4 Reference Road Slope

As reference to the road slope estimations a digital topological map was specially ordered from the Swedish National Road Administration through the National Road Database (NVDB) containing longitude, latitude and altitude measurements along the motorway segment.

The topographical reference map was received as points addressed with longitude, latitude and altitude values. For conversion to road slope the central-difference formula was applied as

$$\frac{dz_k}{ds} \approx \frac{z_{k+1} - z_{k-1}}{s_{k+1} - s_{k-1}} \tag{5.3}$$

with

$$\alpha = \varsigma \arctan(\frac{dz_k}{ds}) \tag{5.4}$$

where z_k is the altitude at point k, s_k is the distance up to point k, ς a constant making radians into percent and α is the road slope.

A 5 km stretch was used as reference road slope. This section was part of a newly constructed motorway from where original construction data was retrieved. In Figure 3.3 the road slope of this section is shown. Difficulties in obtaining data with desired accuracy prevented comparison with longer road segments.

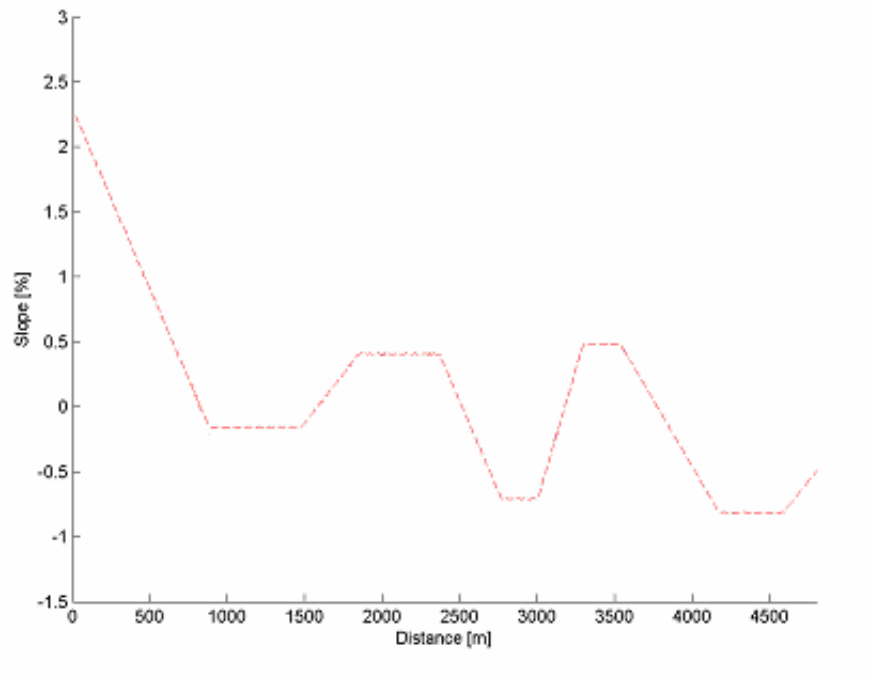

Figure 3.3: Road slope derived from NVDB data.

4 Theory

4.1 State Space Modelling

To estimate the road slope angle a model of the truck's movement is needed. The model is derived from the continuous-time case on the form

$$\dot{x} = f(x,u) \tag{4.1}$$
$$y = Hx \tag{4.2}$$

where f is the non-linear system function and H the linear measurement function. States are chosen as

$$x_1 = z \tag{4.3}$$
$$x_2 = \alpha \tag{4.4}$$

where z equals the road altitude and α is the road slope angle. The measurement vector y is

$$y = \begin{pmatrix} y_1 \\ y_2 \\ y_3 \end{pmatrix} = \begin{pmatrix} x_1 \\ \gamma x_1 \\ x_2 \end{pmatrix} = \begin{pmatrix} 1 & 0 \\ \gamma & 0 \\ 0 & 1 \end{pmatrix} x = Hx \tag{4.5}$$

where y_1 is the altitude measured by the GPS, y_2 the barometric pressure from the pressure sensor and y_3 the road slope estimated by the torque sensor. γ is the conversion rate factor for converting atmospheric pressure to altitude. From Figure 4.1 the state x_1 can be written as

$$x_1 = s \sin x_2 \tag{4.6}$$

where s is distance. The state derivatives then becomes

$$\dot{x}_1 = u \sin x_2 \tag{4.7}$$
$$\dot{x}_2 = 0 \tag{4.8}$$

where u is the vehicle speed over ground. As variations in the slope x_2 are small $\dot{x}_2$ is set to zero. The non-linear state space form now becomes

$$\dot{x} = \begin{pmatrix} u \sin x_2 \\ 0 \end{pmatrix} \tag{4.9}$$
$$y = Hx\,. \tag{4.10}$$

In the time-discrete case equation (4.11) and (4.12) becomes

$$x_{k+1} = x_k + T \begin{pmatrix} u \sin x_2 \\ 0 \end{pmatrix}_k \tag{4.11}$$
$$y_k = Hx_k \tag{4.12}$$

where T is the sampling rate.

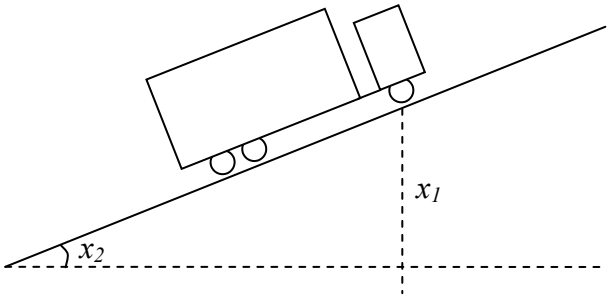

Figure 4.1: System variables

4.2 Observer

To estimate the states from measured inputs and outputs an observer through a feedback loop can be used [17]. Consider the system

$$\dot{x} = f(x,u) \tag{4.13}$$
$$y = Hx\,. \tag{4.14}$$

From equation (4.16) follows that the estimate $\hat{y}$ would be equal to y if the estimate of x would be exactly equal to $\hat{x}$. Thus making the difference

$$y - H\hat{x} \tag{4.15}$$

a degree of how well $\hat{x}$ estimates x. Using (4.17) for feedback purpose gives the estimation equation

$$\dot{\hat{x}} = f(\hat{x},u) + K(y - H\hat{x}) \tag{4.16}$$

which is the observer for the system (4.15) – (4.16).

4.3 Kalman Filter

The Kalman Filter [18] [19] [20] is a way to calculate the observer and is used to minimise measurement and state errors. In this study an extended Kalman Filter (EKF) was used as the state difference equation was non-linear and for potential sensor fusion purpose.

4.3.1 Linear Kalman Filter

The discrete Kalman filter is an estimation method for linear systems in state space form. It is an observer that utilises the stochastic behaviour of process and measurement noise to estimate the state x from measurements y. The system is mathematically formulated on state space form as

$$x_k = Ax_{k-1} + Bu_{k-1} + w_{k-1} \tag{4.17}$$
$$y_k = Hx_k + v_k \tag{4.18}$$

where u_k is the known system input and random variables w_k and v_k representing the process and measurement noise. The variables w_k and v_k are zero mean white noise processes with

$$Q_k = E\left[w_k w_k^T\right] \tag{4.19}$$

$$R_k = E\left[v_k v_k^T\right] \tag{4.20}$$

where Q_k denotes the process noise covariance and R_k the measurement noise covariance. The aim is to find an equation that calculates the state x_k as follows

$$\hat{x}_k = \hat{x}_{k|k-1} + K_k\left(y_k - H_k\hat{x}_{k|k-1}\right). \tag{4.21}$$

Here the notation $\hat{x}_{k|k-1}$ means the estimate of x_k using values up to time *k-1*, y_k is the actual measurement and $H_k\hat{x}_{k|k-1}$ a measurement prediction. The matrix K is chosen to be the gain that minimizes the error in the estimate. K is often called the Kalman gain and is usually chosen as

$$\begin{aligned} K_k &= P_{k|k-1}H_k^T\left(H_k P_{k|k-1}H_k^T + R_k\right)^{-1} \\ &= \frac{P_{k|k-1}H_k^T}{H_k P_{k|k-1}H_k^T + R_k}. \end{aligned} \tag{4.22}$$

The equations for the Kalman filter algorithm is divided into two parts, time update equations and measurement update equations. The time update equations projects the current estimate ahead in time and are given by

$$\hat{x}_{k|k-1} = A_k\hat{x}_{k-1} + B_k u_{k-1} \tag{4.23}$$

$$P_{k|k-1} = A_k P_{k-1}A^T + Q_{k-1} \tag{4.24}$$

where P is the estimate error covariance matrix. The measurement update then adjusts the projected estimate by an actual measurement at that time. This is given by

$$K_k = P_{k|k-1}H_k^T\left(H_k P_{k|k-1}H_k^T + R_k\right)^{-1} \tag{4.25}$$

$$\hat{x}_k = \hat{x}_{k|k-1} + K_k\left(y_k - H_k\hat{x}_{k|k-1}\right) \tag{4.26}$$

$$P_k = \left(I - K_k H_k\right)P_{k|k-1}\,. \tag{4.27}$$

The first equation in the measurement update is to compute the Kalman gain K_k. The next equation is to actually measure the process to obtain y_k, and to then update a state incorporating the measurement. The final equation is to update the error covariance estimate. Initial values for the state estimate x_0 and the error covariance matrix P_0 must be set.

4.3.2 Extended Kalman Filter

In the above section the general problem of trying to estimate the state of a process with a Kalman filter regulated by a linear difference equation was addressed. In the case of this thesis the process to be estimated is non-linear requiring another approach. Here a Kalman filter that linearizes the estimation around the current estimate is useful. This type of Kalman filter is referred to as an extended Kalman filter or EKF. In a similar way to a Taylor series the partial derivatives of the process and measurement functions are used to compute estimates even in the non-linear case. Let's re-examine the system (4.19) and (4.20) in a non-linear case

$$x_k = f\left(x_{k-1}, u_{k-1}, w_{k-1}\right) \tag{4.28}$$

$$y_k = h\left(x_k, v_k\right) \tag{4.29}$$

where the random variables w_k and v_k again are representing the process and measurement noise as in equations (4.19) and (4.20). The functions f and h represent non-linear functions.

To estimate the non-linear process a first order Taylor expansion of (4.30) and (4.31) is performed,

$$x_k \approx \tilde{x}_k + A_k\left(x_{k-1} - \hat{x}_{k-1}\right) + W_k w_{k-1} \tag{4.30}$$

$$y_k \approx \tilde{y}_k + H_k\left(x_k - \tilde{x}_k\right) + V_k v_k \tag{4.31}$$

where x_k and y_k are the actual state and measurement vectors, $\hat{x}_k$ is an estimate of the state at step k, variables w_k and v_k are representing the process and measurement noise and $\tilde{x}_k$ and $\tilde{y}_k$ are the approximate state and measurement vectors

$$\tilde{x}_k = f\left(\hat{x}_{k-1}, u_{k-1}, 0\right) \tag{4.32}$$

$$\tilde{y}_k = h\left(\tilde{x}_k, 0\right). \tag{4.33}$$

The matrices are the Jacobian matrices of partial derivatives as

$$A_{k[i,j]} = \frac{\partial f_{[i]}}{\partial x_{[j]}}\left(\hat{x}_{k-1}, u_{k-1}, 0\right) \tag{4.34}$$

$$W_{k[i,j]} = \frac{\partial f_{[i]}}{\partial w_{[j]}}\left(\hat{x}_{k-1}, u_{k-1}, 0\right) \tag{4.35}$$

$$H_{k[i,j]} = \frac{\partial h_{[i]}}{\partial x_{[j]}}\left(\tilde{x}_k, 0\right) \tag{4.36}$$

$$V_{k[i,j]} = \frac{\partial h_{[i]}}{\partial v_{[j]}}\left(\tilde{x}_k, 0\right). \tag{4.37}$$

The EKF time update equations then becomes

$$\hat{x}_{k|k-1} = f\left(\hat{x}_{k-1}, u_{k-1}, 0\right) \tag{4.38}$$

$$P_{k|k-1} = A_k P_{k-1} A^T + W_k Q_{k-1} W_k^T \tag{4.37}$$

with the measurement update equations

$$K_k = P_{k|k-1} H_k^T \left(H_k P_{k|k-1} H_k^T + V_k R_k V_k^T\right)^{-1} \tag{4.40}$$

$$\hat{x}_k = \hat{x}_{k|k-1} + K_k\left(y_k - h\left(\hat{x}_{k|k-1}, 0\right)\right) \tag{4.41}$$

$$P_k = \left(I - K_k H_k\right) P_{k|k-1}. \tag{4.42}$$

The basic operation of the extended Kalman filter is the same as the linear discrete Kalman filter.

4.4 Altitude and Slope Relations

The relation between altitude and its derivative (slope) is not always easy to picture. The basic features are shown in Figure 4.2 picturing a single hill where z is the altitude of the road and α is the slope of the road. The hill and its slope can be divided into seven main parts.

1. Start of an incline. This section is typically built as an arced segment of second order. This gives the road slope character of a constantly rising slope value.
2. Hill incline. A constant incline gives a constant positive slope value.
3. End of incline. This section is the opposite of 1 giving a constant fall in the road slope value.
4. Top of the hill. The flat area produces a zero slope value.
5. Start of a decent. The parabolic curvature with constantly decreasing slope gives the same result as 3, but on the negative half of the slope graph.
6. Hill decent. Opposite to 2. With a constant drop in altitude the slope value becomes constant and negative.
7. End of decent. Same as 1 but from negative to zero road slope.

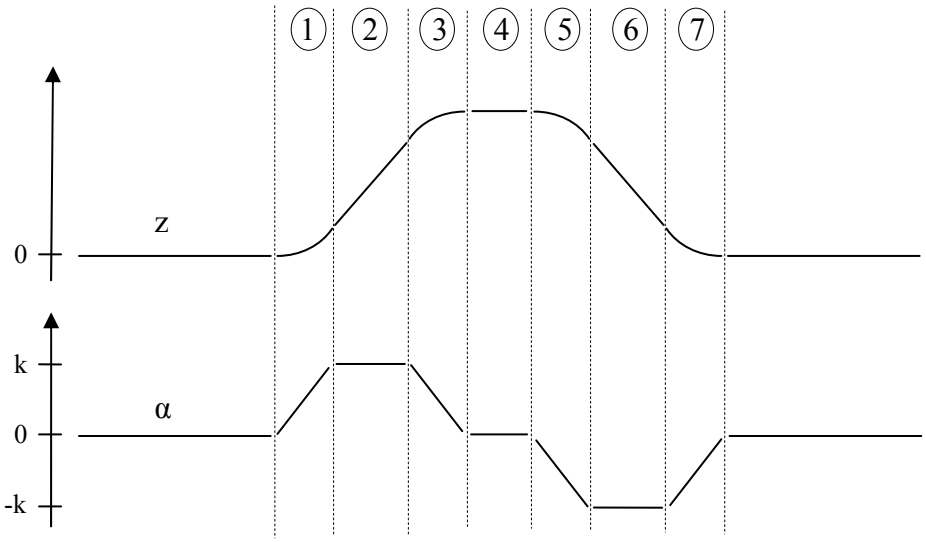

Figure 4.2: Relation between altitude (z) and slope (α).

5 Road Slope Estimation Results

5.1 Model Implementation

As the state equation (4.11) is non-linear the Extended Kalman filter was used. In the time-discrete case the model of the road changes can be described by the non-linear state equation (4.28) and the linear measurement equation (4.18) as

$$x_k = f\left(x_{k-1}, u_{k-1}, w_{k-1}\right) \tag{5.1}$$

$$y_k = Hx_k + v_k \tag{5.2}$$

with matrix H in (5.2) being a 3×3 identity matrix. Equation (5.1) an be described from (4.11) as

$$x_k = f\left(x_{k-1}, u_{k-1}, w_{k-1}\right) = \begin{bmatrix} f_1\left(x_{k-1}, u_{k-1}, w_{k-1}\right) \\ f_2\left(x_{k-1}, u_{k-1}, w_{k-1}\right) \end{bmatrix} = \\ = \begin{bmatrix} (x_1)_{k-1} + u_{k-1}\sin(x_2)_{k-1} \\ (x_2)_{k-1} \end{bmatrix} + w_{k-1}. \tag{5.3}$$

As the state equation is non-linear, (4.30) is applied to linearize an estimate about the equation, giving

$$x_k \approx \tilde{x}_k + A_k\left(x_{k-1} - \hat{x}_{k-1}\right) + W_k w_{k-1} \tag{5.4}$$

where $\tilde{x}_k$ comes from (4.32). A_k and W_k can now be calculated from (4.34) and (4.35).

$$A_k = \frac{\partial f}{\partial x}\left(\hat{x}_{k-1}, u_{k-1}, 0\right) = \begin{bmatrix} \frac{\partial f_1}{\partial x_1} & \frac{\partial f_1}{\partial x_2} \\ \frac{\partial f_2}{\partial x_1} & \frac{\partial f_2}{\partial x_2} \end{bmatrix} = \begin{bmatrix} 1 & u_{k-1}\cos(x_3)_{k-1} \\ 0 & 1 \end{bmatrix} \tag{5.5}$$

$$W_k = \frac{\partial f}{\partial w}\left(\hat{x}_{k-1}, u_{k-1}, 0\right) = \begin{bmatrix} \frac{\partial f_1}{\partial w_1} & \frac{\partial f_1}{\partial w_2} \\ \frac{\partial f_2}{\partial w_1} & \frac{\partial f_2}{\partial w_2} \end{bmatrix} = \begin{bmatrix} 1 & 0 \\ 0 & 1 \end{bmatrix} \tag{5.6}$$

The random variables w_k and v_k in (5.1) and (5.2) are representing the process and measurement noise.

$$w_k = \begin{bmatrix} w_k^z & w_k^\alpha \end{bmatrix}^T \tag{5.7}$$

$$v_k = \begin{bmatrix} v_k^z & v_k^p & v_k^\alpha \end{bmatrix}^T \tag{5.8}$$

The disturbances w_k and v_k are assumed to be independent zero mean white noise processes with normal probability distributions. From (4.19) the noise covariance matrix Q_k can be calculated as

$$\begin{aligned} Q_k = E\left[w_k w_k^T\right] &= E\left[\begin{pmatrix} w_k^z \\ w_k^\alpha \end{pmatrix}\begin{pmatrix} w_k^z & w_k^\alpha \end{pmatrix}\right] = \\ &= \begin{pmatrix} V\left[w_k^z\right] & 0 \\ 0 & V\left[w_k^\alpha\right] \end{pmatrix} \end{aligned} \tag{5.9}$$

with E representing the expectation and V the variance. A diagonal matrix is formed as the disturbances are assumed to be independent, thus having no cross-correlation. In this same manner the noise covariance matrix R_k can be calculated from (4.20) as

$$R_k = \begin{pmatrix} V\left[v_k^z\right] & 0 & 0 \\ 0 & V\left[v_k^p\right] & 0 \\ 0 & 0 & V\left[v_k^\alpha\right] \end{pmatrix}. \tag{5.10}$$

The variances in (5.9) and (5.10) are unknown and therefore have to be estimated. As (5.10) shows, R_k is the variance of the error in the measurements. From the sensor's resolutions, expected accuracies and observations estimated values are initially chosen as

$$V\left[v_k^z\right] = 16 \tag{5.11}$$

$$V\left[v_k^p\right] = 4 \tag{5.12}$$

$$V\left[v_k^\alpha\right] = 0.1. \tag{5.13}$$

The process noise covariance matrix Q_k is chosen as the design parameter matrix. Initially R_k and Q_k are set to constant values. There is no exact right or wrong way of choosing Q_k and R_k. Often good filter performance is obtained by tuning the filter parameters Q_k and R_k manually. Equations (4.38) and (4.39) can now be used for the measurement update to predict the state and covariance estimates from previous time step *k-1* to current time step *k*. Next the linear measurement update equations (4.25) - (4.27) are used to correct the state and covariance estimates with the measurement y_k. In Figure 5.1 a scheme of the Kalman filter operations are shown.

The slope values are now a function of time. Slope as a function of distance is more desired and is achieved by relating each slope value to a distance value from the measured speed at that instant. As the exact same path was driven at all measurements distance values will be equal for each of the runs. To convert measurements relating to distance instead of time and then run the Kalman filter was also performed, but with no significant difference. As the original model with Kalman filter over time has the velocity as input the distance is taken into consideration. Slope estimation was done at 1 Hz sampling rate.

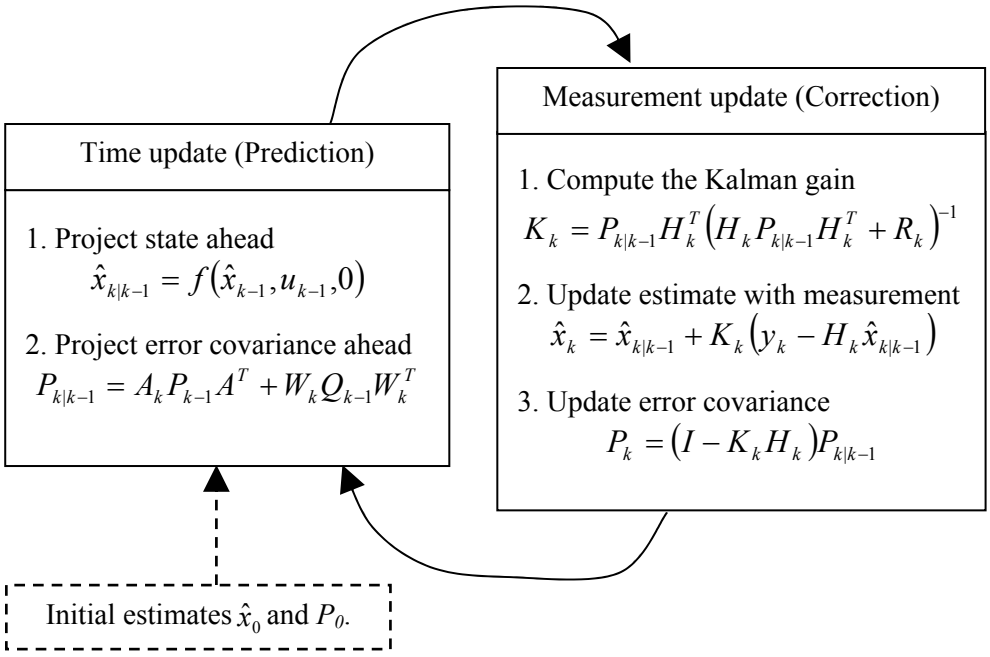

Figure 5.1: Kalman filter operations scheme [19].

5.2 Sensor Evaluation

To determine the characteristics for each of the three sensors a sensor evaluation was carried out. Two key features were considered, the standard deviation and average for the road slope estimation of each sensor. Both features are calculated from the four measurements from each of the two road segment. A signal separation and filter tuning was first performed.

5.2.1 Use of Standard Deviation and Average

Standard deviation

The standard deviation is used as a measure for the stability of the sensor, or how much the sensor readings differ over a number of runs. The standard deviation σ_k is calculated through

$$\sigma_k = \left(\frac{1}{n-1} \sum_{i=1}^{n} \left(q_{i,k} - \bar{q}_k \right)^2 \right)^{\frac{1}{2}} \tag{5.14}$$

where

$$\bar{q}_k = \frac{1}{n} \sum_{i=1}^{n} q_{i,k} \ . \tag{5.15}$$

Here n is the number of runs and q is a $n \times m$ matrix containing m number of elements in the sample. A smaller standard deviation indicates a more stable sensor while a large value indicates a sensor with larger variation between runs.

Average

The average of the four runs is used as a measure of the progressing accuracy of the sensor measurements. Here the standard equation for average (5.15) is used. This will be compared to the reference topographical map received from the NVDB.

5.2.2 Signal Separation

To isolate the behaviour and slope estimation from a single sensor the measurement noise covariance matrix R_k was manually altered. The elements in R_k not corresponding to the sensor of interest were multiplied with a large number (10^{10}) making these signals heavily filtered. From equation (4.25) a very big R_k gives an almost zero K_k implying no feedback in equation (4.26).

For example when only the GPS measurements were of interest the measurement noise covariance matrix R_k was set to

$$R_k = \begin{pmatrix} V\left[v_k^z\right] & 0 & 0 \\ 0 & V\left[v_k^p\right] \times 10^{10} & 0 \\ 0 & 0 & V\left[v_k^\alpha\right] \times 10^{10} \end{pmatrix} \tag{5.16}$$

giving the Kalman gain

$$K_k \approx \begin{pmatrix} K_{11} & 0 & 0 \\ K_{21} & 0 & 0 \end{pmatrix}_k . \tag{5.17}$$

This means that only feedback from the first state (GPS) is considered.

5.2.3 Filter Tuning

As the road slope angle is of main interest the third state in the state space model is considered. Initially the filter was tuned for the signals to achieve best match with the reference slope. The fact with the torque sensor returning invalid slope estimations when wheel brakes are applied was first handled. This was done by giving the element in the measurement noise covariance matrix R_k relating to the slope a big value when the slope values reached its non-valid indication of +13%. From previous section this implies a minimal K_k resulting in a constant slope value. This is illustrated in Figure 5.2.

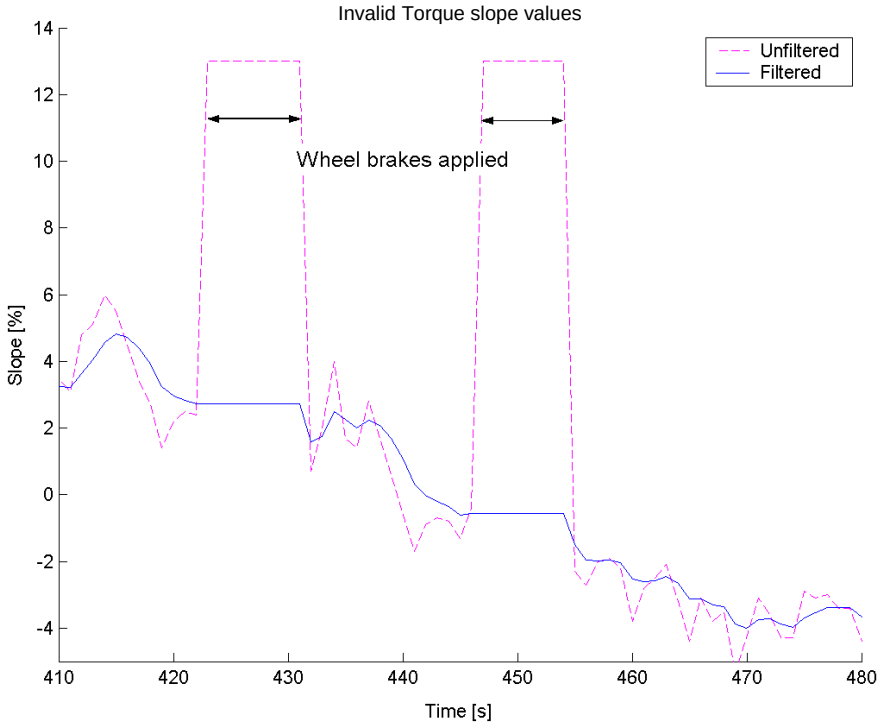

Figure 5.2. Constant slope values when wheel brakes are applied.

In Figures 5.3 – 5.5 the road slope from the well defined section of the reference road is compared to the estimated road slope from averaged measured values of each sensor. Estimated road slope signals are time shifted to agree with the reference curve. An internal pre-filtering of the altitude incorporated in the GPS receiver adds to the time shift of the GPS curve. The time shifts of the GPS, torque sensor and barometer is respectively 12, 10 and 16 seconds.

From Figure 5.3 and Figure 5.4 both the GPS and torque sensor show fairly good matching characteristics while the barometer in Figure 5.5 has problems with the dynamics of the road. This is due to a heavier filtration caused by the lack in resolution of the sensor. After comparing the figures, the GPS estimation (Figure 5.3) appear to show closest match with the reference slope leading to the conclusion that the GPS signal is the signal closest to real values.

As the NVDB data was largely unreliable and with the GPS signal showing best matching characteristics on the short reliable part the GPS signal is from now on used as reference curve. There is no indication to suspect large changing accuracies in the GPS signal as the satellite coverage was satisfactory along both roads at all times.

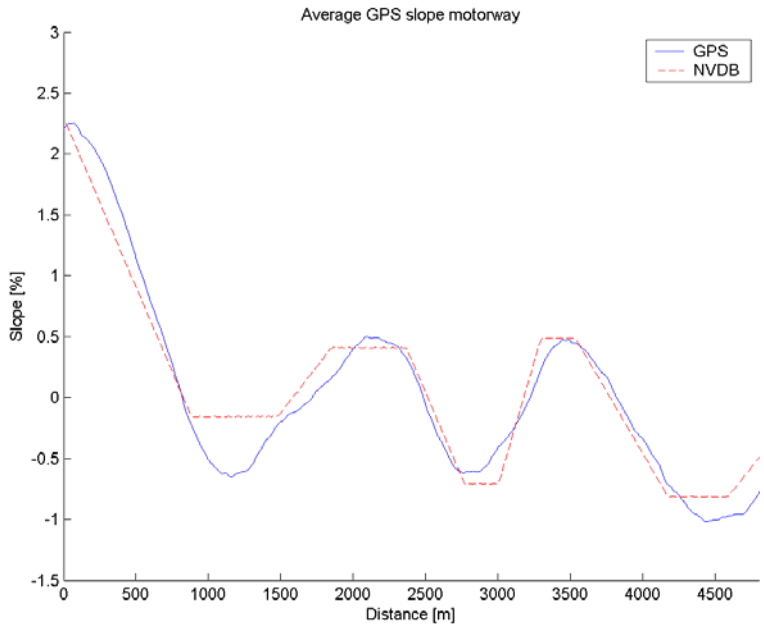

Figure 5.3: Road slope comparison of GPS and NVDB data.

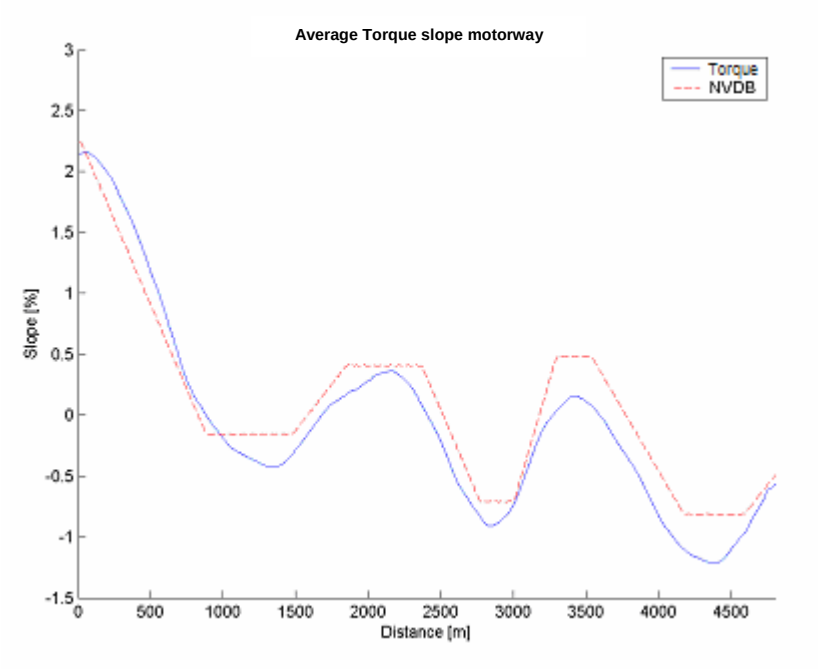

Figure 5.4: Road slope comparison of torque sensor and NVDB data.

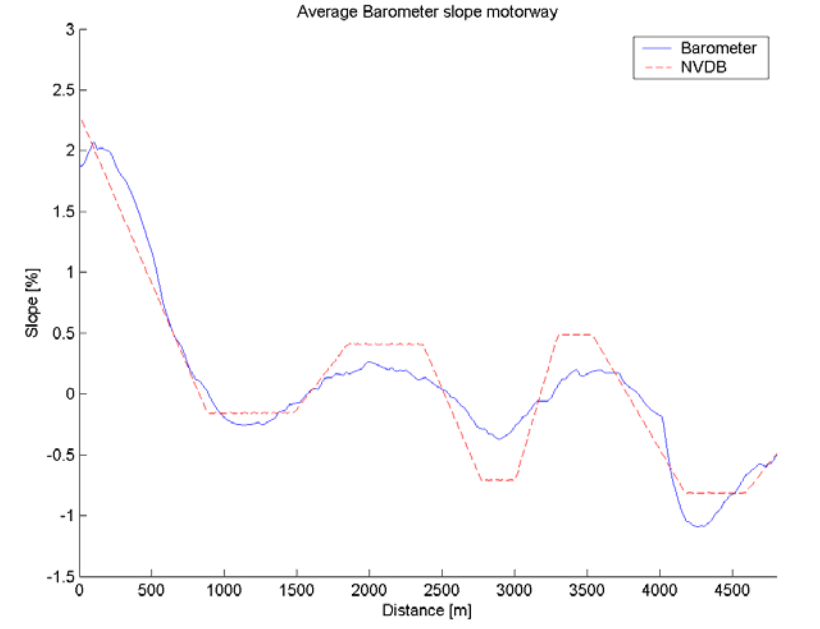

Figure 5.5: Road slope comparison of barometer and NVDB data.

5.3 Results Motorway Segment

5.3.1 Standard Deviation

In Figures 5.6 – 5.8 standard deviation for the motorway segment is presented for each sensor. From the GPS standard deviation in Figure 5.6 a quite evenly distributed deviation is observed. Larger initiating values are due to a motorway on ramp section where satellite visibility momentarily decreased causing larger uncertainties in the altitude measurements. In Figure 5.7 standard deviation for the torque sensor is shown. Irregularities in the beginning and end are due to times with applied wheel brakes. These are times before and after the motorway. The two smaller maxima at around 2×10^4 and 2.8×10^4 meters are caused by variations in the positioning of valleys. This is due to the fact that the slope estimation from the torque sensor is affected by the driving situations of the truck and is for that reason sometimes inconsistent. The Barometer standard deviation in Figure 5.8 shows a quite evenly distributed deviation as the GPS, although with larger values. To get an easier comparison index the average values of the standard deviations are presented in Table 5.1.

The result in Table 5.1 shows that the torque sensor signal has the smallest standard deviation while the barometer has the largest, leading to the conclusion that torque sensor is the most stable sensor for motorway segments.

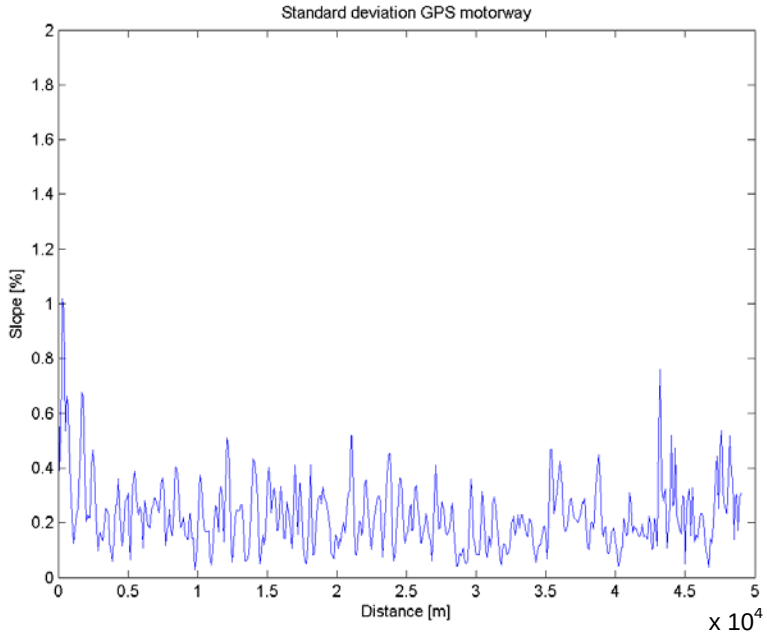

Figure 5.6: Standard deviation for GPS over motorway segment.

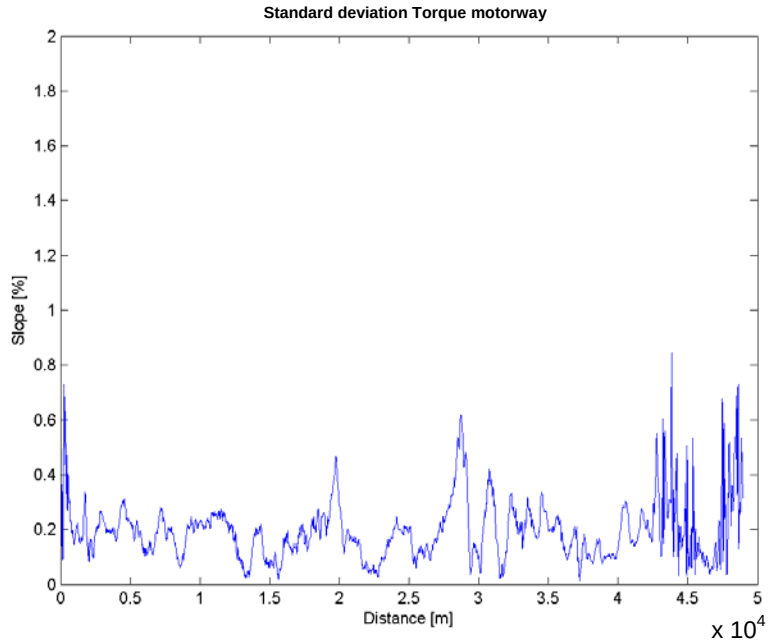

Figure 5.7: Standard deviation for torque sensor over motorway segment.

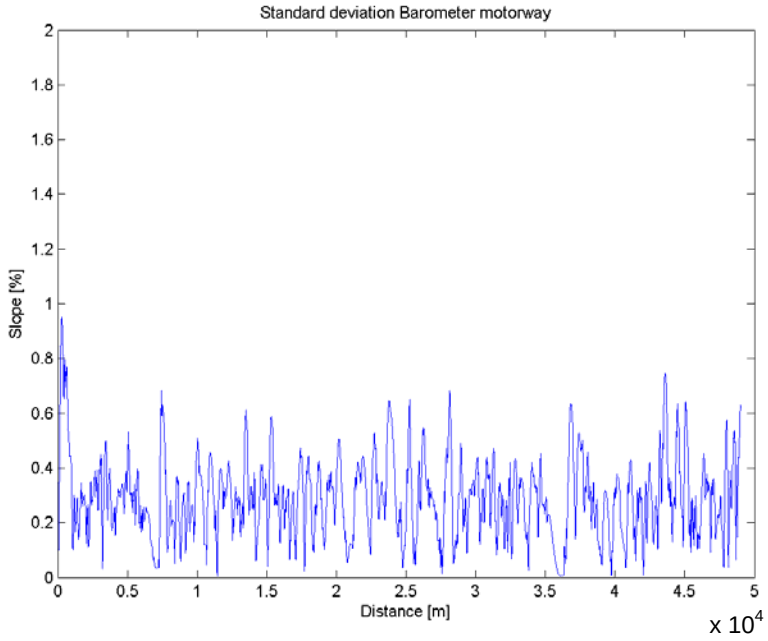

Figure 5.8: Standard deviation for barometer over motorway segment.

	GPS	Torque sensor	Barometer
Average std [%]	0.23	0.19	0.29

Table 5.1: Average standard deviation over motorway.

5.3.2 Average Road Slope

In Figure 5.9 a part of the average torque sensor road slope showing typical characteristics is plotted with the GPS curve as reference. Here a tendency can be observed of sometimes showing a negatively biased slope estimation value. Differences can be observed around 0.7×10^4 and 1.2×10^4 meters. Overall a smooth and reliable curve is observed. In Figure 5.10 the averaged slope estimation from the barometer is presented over the same distance. Here the general result is that the pressure sensor tends to underestimate the road slope magnitude. This is due to increased filtration relating to the lack of resolution in the sensor. If less filtration is desired the number of runs averaged need to be increased. An edginess to the curve can also be observed, which would increase if less filtration is applied. The overall match with the reference curve is not satisfactory with large differences at e.g. around 1.2×10^4 meters.

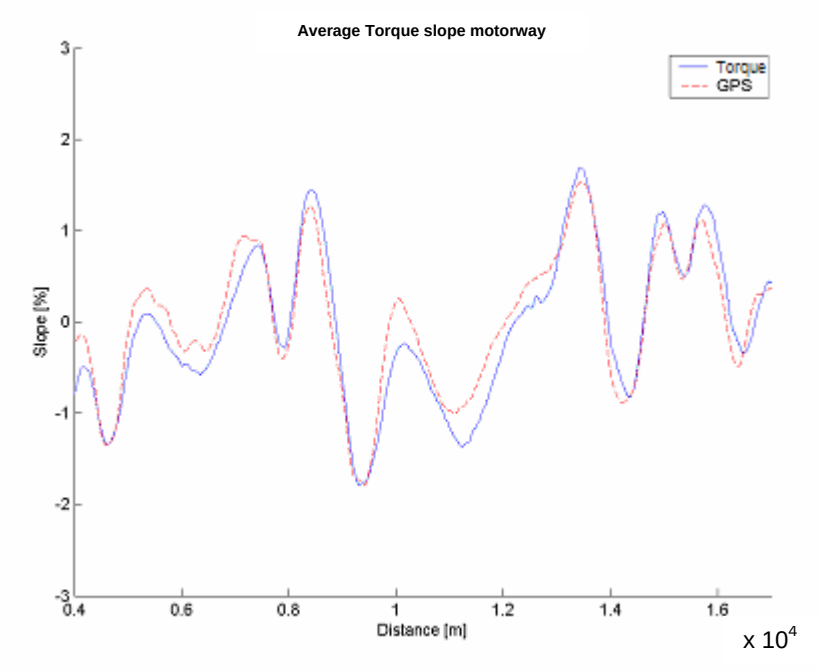

Figure 5.9: Average road slope for torque sensor and GPS over motorway.

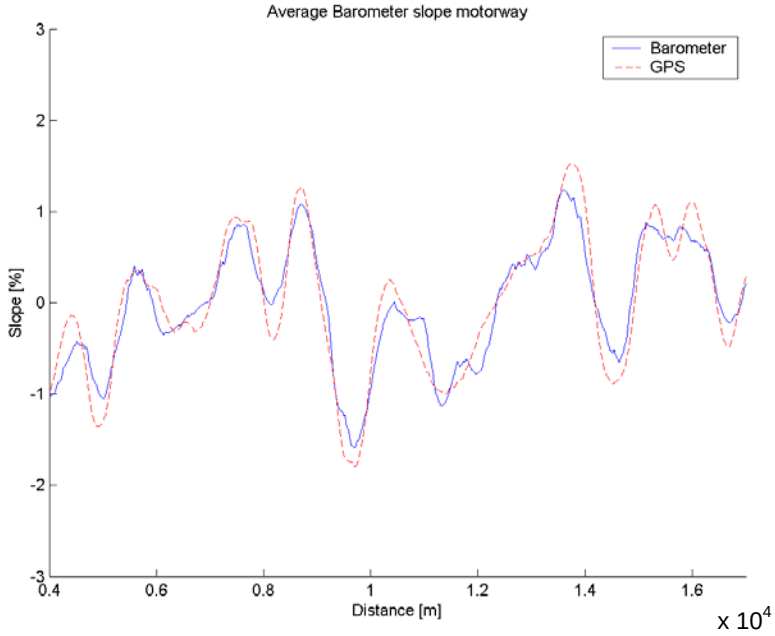

Figure 5.10: Average road slope for Barometer and GPS over motorway.

5.4 Results Main Road Segment

5.4.1 Standard Deviation

In Figure 5.11 – 5.13 the standard deviation for the main road segment is presented. Calculations are done in the same way as for the motorway in section 5.3.1. A table with the average standard deviations are presented in Table 5.2. The order of smallest standard deviation is the same as for the motorway segment. The GPS and torque sensor show comparable deviation values on the much more diverse main road compared to the motorway segment (Table 5.1), while the barometer shows a lower value. The torque sensor still has the lowest value.

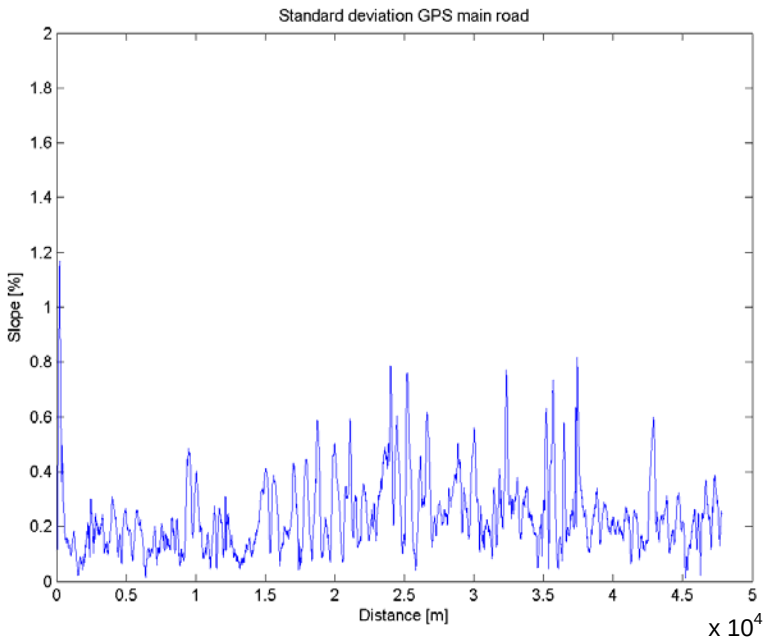

Figure 5.11: Standard deviation for GPS over main road segment.

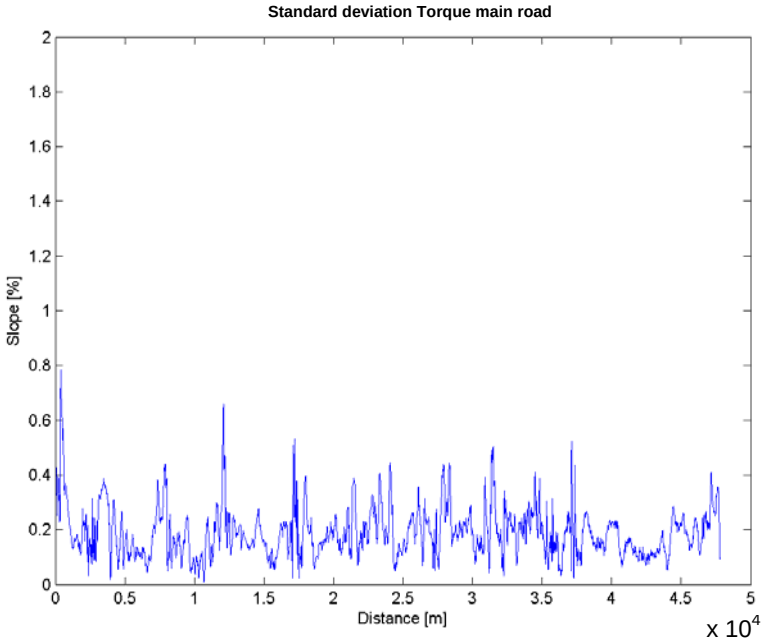

Figure 5.12: Standard deviation for torque sensor over main road segment.

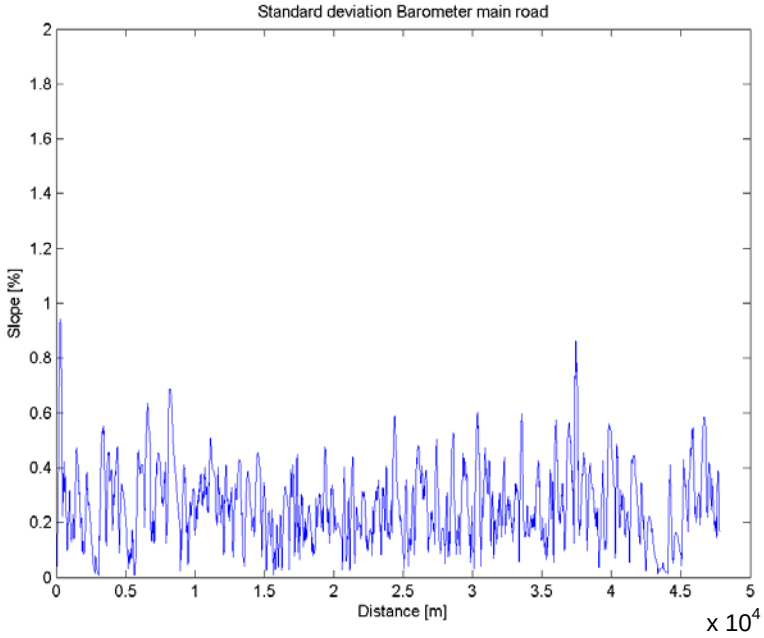

Figure 5.13: Standard deviation for barometer over main road segment.

	GPS	Torque sensor	Barometer
Average std [%]	0.24	0.19	0.26

Table 5.2: Average standard deviation over main road.

5.4.2 Average Road Slope

The average road slope for the main road segment is presented in Figure 5.14 and 5.15. A part of the torque sensor slope estimation showing the typical behaviour is plotted with the reference curve in Figure 5.14. Here similar results to the motorway segment can be observed. A tendency to sometimes show a negatively biased slope estimation value can be seen but with even larger deviation than from the motorway segment (see around 2.2×10^4 m). Figure 5.15 shows the average barometer slope estimation. Also here showing similar results to the motorway segment with the sensor tending to underestimate the road slope magnitude. Both sensors show difficulties in accurately estimating the road slope for the much more diverse and hilly main road.

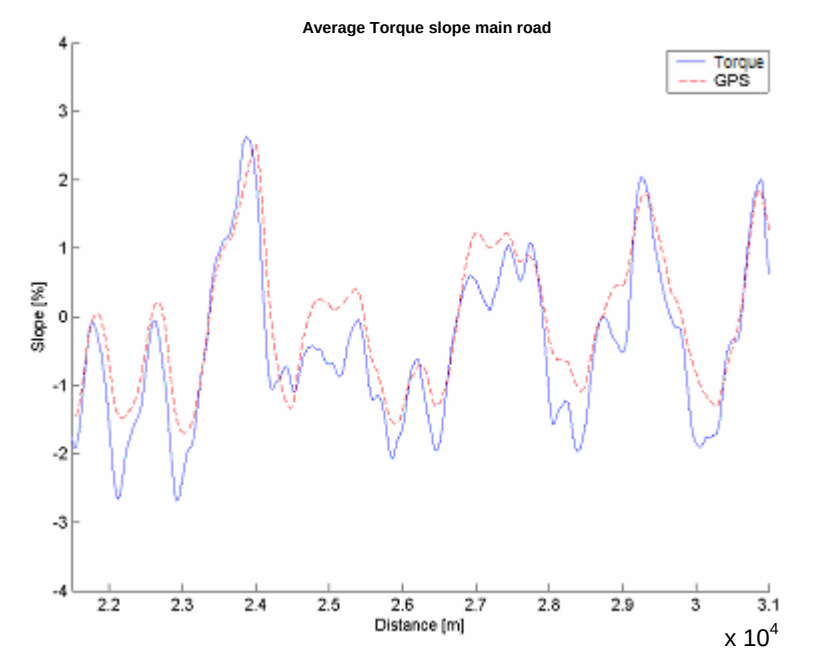

Figure 5.14: Average road slope for torque sensor and GPS over main road.

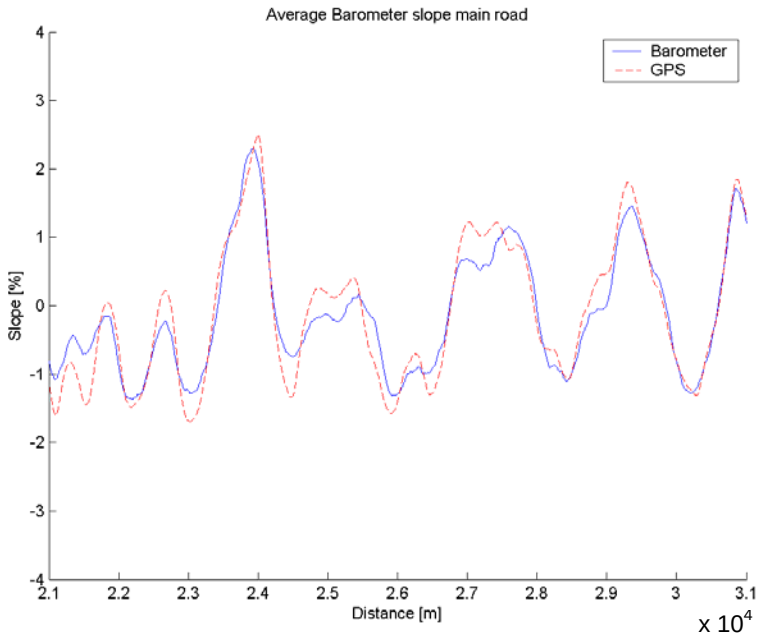

Figure 5.15: Average road slope for Barometer and GPS over main road.

5.5 Accuracy in Opposition to Data Quantity

With the GPS signal proposed as the best signal for estimating the road slope an assessment of the needed accuracy, or resolution, in the signal is carried out. As the signal from the Kalman filter is time variant it is transformed to be distance variant. An equally spaced signal is wanted why an interpolation is performed. The distance between two following points is now the key feature in how large the data quantity becomes. A short distance gives high accuracy with a large data quantity while a large distance gives less accuracy but with a smaller data quantity. A comparison between three different interpolation distances is done. Road slope are interpolated with distances of 1, 20 and 100 meters apart.

In Figure 5.16 a part of the main road section with the biggest deviation between the three curves is shown. A short and steep slope is pictured through its gradient. Here the difference between 1 and 20 meters is small and could be neglected. The difference between the 1 and 100 meters is much larger and is from Figure 5.16 a difference of about 0.6 % incline. In the case of the motorway segment the maximum difference observed

between the 1 and 100 meter interpolation distance resulted in 0.05 % incline, which can be neglected. This gives the result that for the main road a sampling distance of around 20 meters is needed while a distance of 100 meters is enough for the motorway.

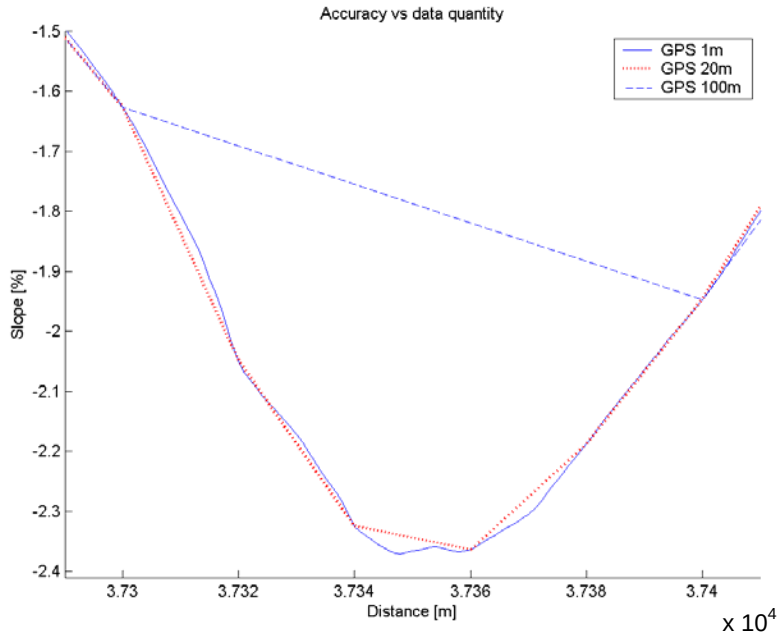

Figure 5.16: GPS road slope estimation on main road with distance resolution 1, 20 and 100 meters.

5.6 Summary Sensor Evaluation

From the sensor evaluation the torque sensor looks to be the most stabile sensor, although showing a tendency to estimate negatively biased slope values. From the average road slope results it also shows that the torque sensor works well on the motorway but not satisfactory on the hillier main roads. The torque sensor also incorporates the problem with times of non-valid estimates when the driver applies wheel breaks, although a minor problem.

The barometer on the other hand shows signs to be very unstable. On the motorway segment the barometer shows unreliable average values, though showing better performance on the main road. The fact that the

barometer also is affected by sudden weather changes and the air-conditioning system is most negative.

The GPS showed equal convincing characteristics on both types of road and had the best match with the reference NVDB curve. A fair standard deviation and no major drawbacks also speak in favour for the GPS. All together the GPS looks to be the most reliable instrument in this study.

As satellite coverage was good along the measured roads influences from low satellite coverage has not been evaluated. Sudden weather changes would affect the barometer reading but has not been examined further.

For the sampling distance the analysis shows that around 20 meters is needed for the main road while a distance of 100 meters is enough for the motorway.

6 Conclusions and Future Work

As information on future three-dimensional road maps was difficult to obtain focus was set on road slope recording. The model derived together with the extended Kalman filter proved to be a functional tool for road slope estimation. An advantage with the Kalman filter is its easy tuning capabilities that can be set to meet different desires. The results from the sensor evaluation showed that the pressure sensor suffered from its low resolution making it difficult to estimate the road slope accurately. With a high standard deviation the signal also tends to show values that differ from day to day. The torque sensor showed to have problems with the quick changing hillier main road while having stable and reliable signals on the motorway. The GPS on the other hand showed equal characteristics on both types of road with good matching characteristics to the reference curve and therefore proved to be the overall most suitable tool for estimating road slope angle. Finally a short assessment of the sampling distance is also carried out. Results showed that for the main road a sampling distance of around 20 meters is needed while a distance of 100 meters is enough for the motorway.

A big issue that came up during the project was the task to find a reliable source to obtain a true reference topographical map for the measured roads. This turned out to be more difficult than expected. Expensive high accuracy GPS equipment was first used in believes that it would accurately depict the travelled road. Unfortunately this GPS suffered from extensive influences from satellite drop outs. Then a digital topological map of the specific road was specially ordered from the Swedish National Road Administration (SNRA) in hopes that this source

would be more accurate. As discussed in section 3.4 this was sadly not true. As the SNRA looked to have some parts of the road network measured with high accuracy these parts have to primarily be used for the measuring experiments in future works. This way the model and the estimations can be properly evaluated.

As Kalman filtering is applied and several sensors are used for the same purpose sensor fusion is a natural step. To investigate if all three sensors together could give a more accurate estimation is a desire which from lack of time was not examined further.

A significant task before having a complete system with look-ahead possibilities is the navigational part with saving and retrieving of the slope information. To be able to look-ahead and predict coming slopes a dynamic map database has to be developed with possibility to update, write and read from.

7 Bibliography

[1] Tony Sandberg. *Heavy Truck Modeling for Fuel Consumption Simulation and Measurements*. Licenciate Thesis, Department of Electrical Engineering, Linköping University, Sweden, 2001.

[2] Niklas Petterson and Karl Henrik Johansson. Optimal Control of the Cooling System in Heavy Vehicles. Proceedings of the IFAC Symposium on *Advances in Automotive Control*, Salerno, Italy, pages 115-120, Apr. 2004.

[3] Mattias Åsbogård, Filip Edström, Johan Bringhed, Mikael Larsson and Jonas Hellgren. Evaluating Potential of Vehicle Auxiliary System Coordination Using Optimal Control, 7th International Symposium on *Advanced Vehicle Control*, Arnhem, Netherlands, pages 701-706, Aug. 2004.

[4] Johan Jonsson and Zandra Jansson. Fuel optimized predictive following in low speed conditions. Proceedings of the IFAC Symposium on *Advances in Automotive Control*, Salerno, Italy, pages 134-139, Apr. 2004.

[5] Anna Wingren. *Fordonsreglering med framförhållning*. Master Thesis, Linköping University, Sweden, 2005.

[6] Frank Lattemann, Konstantin Neiss, Stephan Terwen and Thomas Connolly. The Predictive Cruise Control – A System to Reduce Fuel

Consumption of Heavy Duty Trucks. *SAE Technical Paper Series* (2004-01-2616), 2004.

[7] DaimlerChrysler, Hightech Report, pages 52-53, 2/2003.

[8] Hong S. Bae, Jihan Ryu and J. Christian Gerdes. Road Grade and Vehicle Parameter Estimation for Longitudinal Control Using GPS, *IEEE, ITS 2001*, Oakland, CA, August 25-29, 2001.

[9] Ardalan Vahidi, Anna Stefanopoulou and Huei Peng. Experiments for Online Estimation of Heavy Vehicle's Mass and Time-Varying Road Grade. *Proceedings of the ASME International Mechanical Engineering Congress and Exposition*, Washington, D.C, November 2003.

[10] Peter Lingman and Bengt Schmidtbauer. *Road Slope and Vehicle Mass Estimation Using Kalman Filtering*. Department of Chassis Engineering, Volvo Truck Corporation.

[11] David Andersson and Johan Fjällström. *Vehicle Positioning with Map Matching Using Integration of a Dead Reckoning System and GPS*. Master Thesis, Linköping University, Sweden, 2004.

[12] Jon Kronander. *Robust Automotive Positioning: Integration of GPS and Relative Motion Sensors*. Master Thesis, Linköping University, Sweden, 2004.

[13] Scania Interactor 500 pamphlet. Scania Fleet Management. Edition 04.04 enXX1595587.

[14] µ-blox TIM GPS Receiver Macro-Component data sheet. Doc id: GPS.G2-MS2-01001-E, 2001

[15] ANT 72488-1 Product Sheet. Smarteq Wireless AB.

[16] Motorola Freescale Semiconductor, Inc. Technical datasheet for MPXA6115A.

[17] Torkel Glad and Lennart Ljung. *Reglerteknik. Grundläggande teori.* Studentlitteratur, 2nd edition, 1989

[18] Monson H. Hayes. *Statistical Digital Signal Processing and Modelling*. John Wiley & Sons, Inc. 1996

[19] Greg Welch and Gary Bishop. *An Introduction to the Kalman Filter*. TR 95-041, 2004

[20] Håkan Hjalmarsson and Björn Ottersten. *Lecture notes in adaptive signal processing*. Royal Institute of Technology. 2002

[21] μ-blox TIM GPS Receiver Macro-Component Protocol Specification, Doc id: GPS.G2-X-01003-E1, 2003

Appendix A: GPS Data Format

The specification defining e.g. GPS receiver communication is called NMEA, which stands for National Marine Electronics Association. Information about position, velocity, heading, time and much more can be extracted from the NMEA sentences. The NMEA sentences are presented at the receiver in the form of ASCII comma-delimited message strings containing different types of information. The first word in the string, called a data type, defines the interpretation of the rest of the sentence. Each data type would have its own unique interpretation and is defined in the NMEA standard. The GPS receiver used in this study outputs six different NMEA data types, two of which were read and used. On the next two pages an extract from [21] giving an explanation on these two data types is presented.

A.1 Global Positioning System Fix Data, GGA

Latitude, longitude, number of satellites used and altitude were extracted from the GGA message strings. Following is an example GGA message string

$GPGGA,163409.348,5916.4824,N,01707.3605,E,1,10,1.2,26.9,M,,,,0000*36

Table A.1 below contains an interpretation of this message.

Name	Format	Example	Description
Message ID	string	$GPGGA	GGA protocol header
UTC Time	hhmmss.sss	163409.348	Current time
Latitude	ddmm.mmmm	5916.4824	Degrees + minutes
N/S Indicator	character	N	N=north or S=south
Longitude	dddmm.mmmm	01707.3605	Degrees + minutes
E/W indicator	character	E	E=east or W=west
Position Fix Indicator	1 digit	1	Range 0 to 3
Satellites Used	numeric	10	Range 0 to 12
HDOP	numeric	1.2	Horizontal Dilution of Precision
MSL Altitude	numeric	26.9	Unit in meters
Units	character	M	Stands for "meters"
Geoid Separation	blank		Not used
Units	blank		Not used
Age of Differential Corrections	numeric		Blank fields when DGPS is not used. Unit in seconds
Diff. Ref. Station ID	numeric	0000	
Checksum	hexadecimal	*36	

Table A.1: GGA data format

A.2 Recommended Minimum Specific GNSS Data, RMC

Speed over ground was extracted from the RMC message strings. Following is an example RMC message string

$GPRMC,163409.348,A,5916.4824,N,01707.3605,E,46.97,308.49,061204,,*3E

Table A.2 below contains an interpretation of this message.

Name	Format	Example	Description
Message ID	string	$GPRMC	RMC protocol header
UTC Time	hhmmss.sss	163409.348	Current time
Status	character	A	A=data valid or V=data invalid
Latitude	ddmm.mmmm	5916.4824	Degrees + minutes
N/S Indicator	character	N	N=north or S=south
Longitude	dddmm.mmmm	01707.3605	Degrees + minutes
E/W indicator	character	E	E=east or W=west
Speed Over Ground	numeric	46.97	knots
Course Over Ground	numeric	308.49	degrees
Date	ddmmyy	061204	Current date
Magnetic Variation	blank		Not used
Checksum	hexadecimal	*3E	

Table A.2: RMC data format